The winter anomaly in the middle-latitude *F* region during the solar minimum period observed by the Constellation Observing System for Meteorology, Ionosphere, and Climate

W. K. Lee,[1,2] H. Kil,[3] Y.-S. Kwak,[1] Q. Wu,[4] S. Cho,[1] and J. U. Park[1]

Received 14 June 2010; revised 19 October 2010; accepted 21 October 2010; published 4 February 2011.

[1] The winter anomaly (or seasonal anomaly) at middle latitudes is a phenomenon during which the daytime plasma density at the *F*-peak height (NmF_2) is greater in winter than in summer. Radio occultation measurements from the Constellation Observing System for Meteorology, Ionosphere, and Climate (COSMIC) satellites provide a new data source for study of the winter anomaly on a global scale. In this study we investigate the altitude, local time, latitude, longitude, and hemispheric variations of the electron density in the middle-latitude ionosphere by analyzing the COSMIC data measured in 2007 during a magnetically quiet period ($Kp \leq 3$). The seasonal mean behavior of the NmF_2 obtained from COSMIC data shows the occurrence of the winter anomaly feature during 0800–1600 LT in the Northern Hemisphere but not in the Southern Hemisphere. The intensity of the winter anomaly is variable with longitude, and a more intense winter anomaly is likely to occur at longitudes closer to the magnetic pole. At northern middle latitudes, a greater electron density in the winter than in the summer occurs in the narrow altitude range near the *F*-peak height. Except for the winter anomaly feature at northern middle latitudes, the electron density at middle latitudes is greater during the summer than during the winter in both hemispheres.

Citation: Lee, W. K., H. Kil, Y.-S. Kwak, Q. Wu, S. Cho, and J. U. Park (2011), The winter anomaly in the middle-latitude *F* region during the solar minimum period observed by the Constellation Observing System for Meteorology, Ionosphere, and Climate, *J. Geophys. Res.*, *116*, A02302, doi:10.1029/2010JA015815.

1. Introduction

[2] Annual or seasonal behaviors of the ionospheric plasma density that deviate from the solar zenith angle dependence are classified into "winter anomaly," "annual anomaly," and "semiannual anomaly." The winter anomaly (also called the seasonal anomaly), often observed at middle latitudes, is a phenomenon during which the daytime electron density at *F*-peak height (NmF_2) is greater in winter than in summer. The annual anomaly (also called the annual asymmetry (AI) or nonseasonal anomaly) is a phenomenon during which NmF_2 combined from both hemispheres is greater during the December solstice than during the June solstice. The semiannual anomaly is a phenomenon during which the NmF_2 is greater during equinoxes than during solstices. Since the first report of the annual anomaly phenomenon by *Berkner and Wells* [1938], characteristics of the ionospheric anomalies and their driving mechanisms have been extensively investigated using ground- and space-based observations and carrying out model simulations [*Yonezawa and Arima*, 1959; *King*, 1961; *Rishbeth and Setty*, 1961; *Duncan*, 1969; *Yonezawa*, 1971; *Torr and Torr*, 1973; *Mayr et al.*, 1978; *Millward et al.*, 1996; *Balan et al.*, 1997; *Rishbeth*, 1998; *Su et al.*, 1998; *Rishbeth et al.*, 2000; *Zou et al.*, 2000; *Mendillo et al.*, 2005; *Pavlov and Pavlova*, 2005, 2009; *Rishbeth and Müller-Wodarg*, 2006; *Zhao et al.*, 2007; *Zeng et al.*, 2008; *Liu et al.*, 2009; *Pavlov et al.*, 2010].

[3] The annual anomaly has been studied using ground ionosonde NmF_2 data [*Yonezawa and Arima*, 1959; *Yonezawa*, 1971; *Torr and Torr*, 1973; *Rishbeth et al.*, 2000; *Zou et al.*, 2000; *Rishbeth and Müller-Wodarg*, 2006], total electron content (TEC) data [*Titheridge and Buonsanto*, 1983; *Mendillo et al.*, 2005; *Zhao et al.*, 2007], and NmF_2 retrievals from the Constellation Observing System for Meteorology, Ionosphere, and Climate (COSMIC) radio occultation measurements [*Zeng et al.*, 2008; *Liu et al.*, 2009]. The annual anomaly also exists in the topside at low latitudes as observed by the Hinotori [*Su et al.*, 1998] and COSMIC [*Liu et al.*, 2009] satellites. Variation of the solar flux onto the Earth due to variation in the Sun-Earth distance (perihelion in the December solstice and aphelion in the June solstice) causes

[1]Korea Astronomy and Space Science Institute, Daejeon, Korea.
[2]Also at University of Science and Technology, Daejeon, Korea.
[3]The Johns Hopkins University Applied Physics Laboratory, Laurel, Maryland, USA.
[4]High Altitude Observatory, National Center for Atmospheric Research, Boulder, Colorado, USA.

0148-0227/11/2010JA015815

the annual anomaly in NmF_2, but the observed intensity of the annual anomaly (30% NmF_2 difference between the December and the June solstices) far exceeds the 7% difference predicted by the annual variation of the Sun-Earth distance [*Rishbeth and Müller-Wodarg*, 2006]. The seasonal differences in the thermospheric neutral composition [e.g., *Mendillo et al.*, 2005; *Rishbeth and Müller-Wodarg*, 2006] and the magnetic field configuration [*Zeng et al.*, 2008] are suggested to be additional drivers of the annual anomaly, but the observed intensity of the annual anomaly has not yet been fully explained by any mechanism.

[4] The semiannual anomaly is known to be pronounced at low latitudes and at southern middle latitudes during low solar activity [*Yonezawa*, 1971; *Torr and Torr*, 1973]. *Millward et al.* [1996] explained the longitudinal and hemispheric variation of the semiannual anomaly by the combined effect of solar zenith angle and offset of the geographic pole from the magnetic pole. In the region far from the magnetic pole the neutral composition change associated with energy deposition into the auroral region is small. In that region the ionospheric plasma density is primarily influenced by the solar zenith angle. The effect of the solar zenith angle on the ionospheric plasma density exceeds the effect of neutral composition during equinox and causes the greater plasma density during equinox than during solstices. *Fuller-Rowell* [1998] proposed that the semiannual variation of the neutral composition is caused by the seasonal difference in atmospheric mixing induced from the global thermospheric circulation. Asymmetric hemispheric heating of the atmosphere during solstices induces the global-scale interhemispheric thermospheric circulation [*Fuller-Rowell*, 1998; *Rishbeth and Müller-Wodarg*, 1999; *Rishbeth et al.*, 2000]. In this situation heavy molecular gases are stirred up and their number density increases in the *F* region (decrease in the ratio of oxygen number density to molecular nitrogen number density; O/N_2 ratio) during solstices. The solar heating is symmetric in equinoxes and the turbulent mixing is relatively weaker compared to that in solstices. As a result, the O/N_2 ratio is greater during equinox than during solstices and produces the semiannual anomaly in thermospheric neutral composition [*Fuller-Rowell*, 1998].

[5] The winter anomaly has been investigated using NmF_2 data from ground ionosondes [*Yonezawa*, 1971; *Torr and Torr*, 1973; *Zou et al.*, 2000; *Yu et al.*, 2004; *Rishbeth and Müller-Wodarg*, 2006; *Pavlov and Pavlova*, 2009; *Pavlov et al.*, 2010]. *Torr and Torr* [1973] provided the global map of the winter anomaly using NmF_2 data from worldwide ionosonde stations. Their results show that the winter anomaly is more pronounced during the solar maximum period and in the Northern Hemisphere than it is during the solar minimum period and in the Southern Hemisphere. The results of *Torr and Torr* [1973] may not determine the intensity of the winter anomaly accurately because they did not exclude the data during magnetically disturbed periods [*Pavlov and Pavlova*, 2009]. However, the TEC data derived from the Ocean Topography Experiment (TOPEX) satellite show similar hemispheric and solar cycle dependence of the winter anomaly during the magnetically quiet condition (mean $Kp \sim 1.7$) [*Jee et al.*, 2004]. Observations made by the middle and upper atmosphere (MU) radar at Shigaraki (34.85°N, 136.10°E) in Japan show the gradual disappearance of the winter anomaly feature with an increase in altitude above the *F*-peak height [*Balan et al.*, 1998, 2000; *Kawamura et al.*, 2002]. The winter anomaly is known to be associated with the seasonal and hemispheric change in the thermospheric neutral composition [*King*, 1961; *Rishbeth and Setty*, 1961; *Lumb and Setty*, 1976; *Rishbeth*, 1998; *Rishbeth and Müller-Wodarg*, 1999, 2006; *Rishbeth et al.*, 2000, 2004; *Yu et al.*, 2004]. The summer-to-winter interhemispheric wind is suggested to be the source of the neutral composition change [*King*, 1964]. *Duncan* [1969] discussed the seasonal and stormtime behavior of the *F* layer in association with the neutral composition change that resulted from the global thermospheric wind circulation. The seasonal change in neutral composition has been identified by ground-based radar and satellite observations [*Alcaydé et al.*, 1974; *Hedin and Alcaydé*, 1974; *Mendillo et al.*, 2005]. The seasonal variation of the vibrationally excited N_2 and O_2 number densities owing to higher vibrational temperature in winter than in summer [*Thomas*, 1968; *Strobel and McElroy*, 1970; *Pavlov and Pavlova*, 2005], and of the electronically excited O^+ ion number density [*Pavlov and Pavlova*, 2009], also contributes to the winter anomaly in the *F* layer. However, the contribution of the vibrationally excited molecular gases to the *F*-layer winter anomaly is 20%–40% [*Torr et al.*, 1980; *Pavlov and Pavlova*, 2005]. This rate decreases with solar activity [*Pavlov and Pavlova*, 2009].

[6] Our knowledge of the winter anomaly obtained from the ground observations of NmF_2 and TEC is limited to areas over continents (mostly in the Northern Hemisphere). Ionospheric observations by incoherent scatter radar (ISR) provide rich information on the ionosphere at local regions, but there are no ISR observations at middle and high latitudes in the Southern Hemisphere. Study of the winter anomaly using NmF_2 and TEC data limits our knowledge of the anomalous seasonal behavior of the ionosphere to the *F*-peak height; investigation of the seasonal behavior of the ionosphere below and above the *F*-peak height is necessary to identify the altitudinal range where the winter anomaly phenomenon occurs. Radio occultation measurements from COSMIC satellites provide a new data source for the investigation of temporal and spatial variability of the winter anomaly on a global scale and the altitudinal range at which the anomalous feature occurs. Longitudinal and altitudinal variations in the annual and winter anomalies have been deduced from global maps of the COSMIC data in previous studies [*Zeng et al.*, 2008; *Liu et al.*, 2009], but these studies were limited to a noon time frame, with an emphasis on the equatorial ionization anomaly (EIA). There have been no dedicated studies of the middle-latitude winter anomaly using the COSMIC data.

[7] In this study we examine the variation of the winter anomaly feature with hemisphere, local time, altitude, latitude, and longitude during low-solar-activity periods by analyzing the COSMIC data for the year 2007. The electron density profiles with height provided by COSMIC enable us to determine the altitudinal range at which the anomalous behavior occurs. In section 2 we briefly describe the COSMIC data. In section 3 we examine the variation in the winter anomaly feature with latitude, local time, longitude, and altitude by analyzing the COSMIC data. COSMIC results are validated by comparison with ionosonde data. In section 4

we discuss the driving mechanisms of the winter anomaly at middle latitudes. Conclusions are given in section 5.

2. COSMIC Data Description

[8] COSMIC consists of six satellites launched into a circular orbit on 15 April 2006. Currently, the satellite orbits are at an altitude of 800 km with an inclination angle of 72°. Longitudinal separation between the satellites is 30°. Radio occultation measurements from the Global Positioning System (GPS) occultation experiment (GOX) payload [*Lei et al.*, 2007] provide about 1500–2300 electron density profiles per day in the 50 to 800 km altitude range. Detailed descriptions of retrieval of the electron density from the GPS radio occultation data is provided and *Lee et al.* [2007] and *Lei et al.* [2007]. COSMIC data are available from the COSMIC Data Analysis and Archival Center (http://cosmic-io.cosmic.ucar.edu/cdaac/).

[9] COSMIC data arrays are produced as a function of geographic longitude, geographic latitude, local time, and altitude, with bin sizes of 5°, 5°, 1 h, and 5 km, respectively. Later, the geographic latitude is converted into the magnetic latitude. COSMIC data arrays are produced using the data from 2007 under $Kp \leq 3$. The year 2007 was in the decreasing phase of the solar cycle close to the solar minimum (annual average $F_{10.7}$ index = 73). Observations in January and December 2007 are used as representative of the December solstice, and observations in June and July 2007 are used as representative of the June solstice. We used the data from January 2007 and 2007 instead of during December 2006 and January 2007 to minimize the solar cycle effect. The mean $F_{10.7}$ indexes during the December and June solstices in 2007 were 78 and 75, respectively. NmF_2 shows a linearly increasing trend with an increase in $F_{10.7}$ index [*Oliver et al.*, 2008]. The difference in the $F_{10.7}$ indexes that we inferred from the result of *Oliver et al.* [2008] causes about a 2% difference in NmF_2 during the December and June solstices in 2007. Figure 1 shows the longitudinally integrated number of the COSMIC data as a function of local time (1 h bin) and magnetic latitude (20° bin) during the December (Figures 1a and 1b) and June (Figures 1c and 1d) solstices. The data distribution is not even with local time during the December solstice. Noontime measurements at northern latitudes in December are rare and statistically underrepresented compared to measurements at other times, but note that the number of noontime data points at northern latitudes in December is not that small (95). The observation of similar climatology of the middle-latitude ionosphere from the analysis of COSMIC data in 2007 and 2008 (2008 results were not shown) indicates that the relatively small number of data near noontime at northern latitudes in December does not cause any bias in our results.

3. Results

[10] The global morphology of the ionosphere is examined by averaging the data with magnetic longitude. Figure 2 shows the electron density distribution at the F-peak height (left) and at a 500 km altitude (right) as a function of magnetic latitude during the December (Figures 2a and 2d) and June (Figures 2b and 2e) solstices. A comparison of Figures 2a and 2b shows that the daytime NmF_2 at low latitudes is greater during the December solstice than during the June solstice. EIAs are developed during the day at the F-peak height. During the December solstice (Figure 2a), the EIA appears earlier in the morning and disappears earlier in the afternoon at northern magnetic latitudes compared to its appearance at southern magnetic latitudes. This trend is reversed in the hemisphere during the June solstice. If the formation of the EIA is controlled purely by vertical plasma drift, the EIA may maintain hemispheric symmetry. The hemispheric difference in the EIA morphology indicates that other factors such as neutral winds, neutral composition, and solar zenith angle affect the formation of the EIA. Because the EIA is a dominant feature in the density plots, seasonal and hemispheric variations of the electron density are not clearly visible at middle latitudes. Figure 2c presents the NmF_2 difference between the December and the June solstices normalized by the density during the December solstice (DEC –JUN)/DEC. The density difference map shows that the NmF_2 at southern magnetic latitudes is greater during the December solstice (southern summer) than during the June solstice (southern winter) at all local times. At northern magnetic latitudes the NmF_2 during daytime (0800–1600 LT) is greater during the December solstice (northern winter) than during the June solstice (northern summer). Thus the winter anomaly feature appears during daytime at northern magnetic latitudes but not at southern magnetic latitudes. The absence of the winter anomaly feature in the Southern Hemisphere may be related to the weakening of the winter anomaly during the decreasing phase of the solar cycle. Reductions in the intensity and spatial range of the winter anomaly were identified during low-solar-activity periods in previous studies [*Torr and Torr*, 1973; *Jee et al.*, 2004].

[11] We note that the anomalous behavior at middle latitudes is not purely described by the winter anomaly; strictly speaking, our figures present the sum of the winter and annual anomalies. The contribution of the annual anomaly makes the winter anomaly feature appear stronger in the Northern Hemisphere and weaker (or disappear) in the Southern Hemisphere. The intensity of the annual anomaly is examined using the AI index defined by *Rishbeth and Müller-Wodarg* [2006]:

$$\mathrm{AI} = \frac{\mathrm{Nm}F_2(N+S)_{\mathrm{Dec}} - \mathrm{Nm}F_2(N+S)_{\mathrm{Jun}}}{\mathrm{Nm}F_2(N+S)_{\mathrm{Dec}} + \mathrm{Nm}F_2(N+S)_{\mathrm{Jun}}}, \quad (1)$$

where N and S indicate the Northern and Southern Hemispheres, respectively. Using the COSMIC NmF_2 data at 0°–60° magnetic latitude, we obtained an AI index of 0.11 (December/June ratio: 1.23). The AI index obtained by *Mendillo et al.* [2005], using the global GPS TEC data for 2002, was 0.15 (December/June ratio: 1.35). The AI index obtained by *Zeng et al.* [2008], using the COSMIC NmF_2 in 2006, was 0.14 (December/June ratio: 1.3). A comparison of the AI indexes in 2002, 2006, and 2007 shows that the AI index decreases with a decrease in solar activity. However, the small change in the AI index does not prove the solar cycle dependence of the intensity of the annual anomaly. *Yonezawa* [1971] suggested that the annual anomaly gets stronger with a decrease in solar activity, but *Rishbeth and*

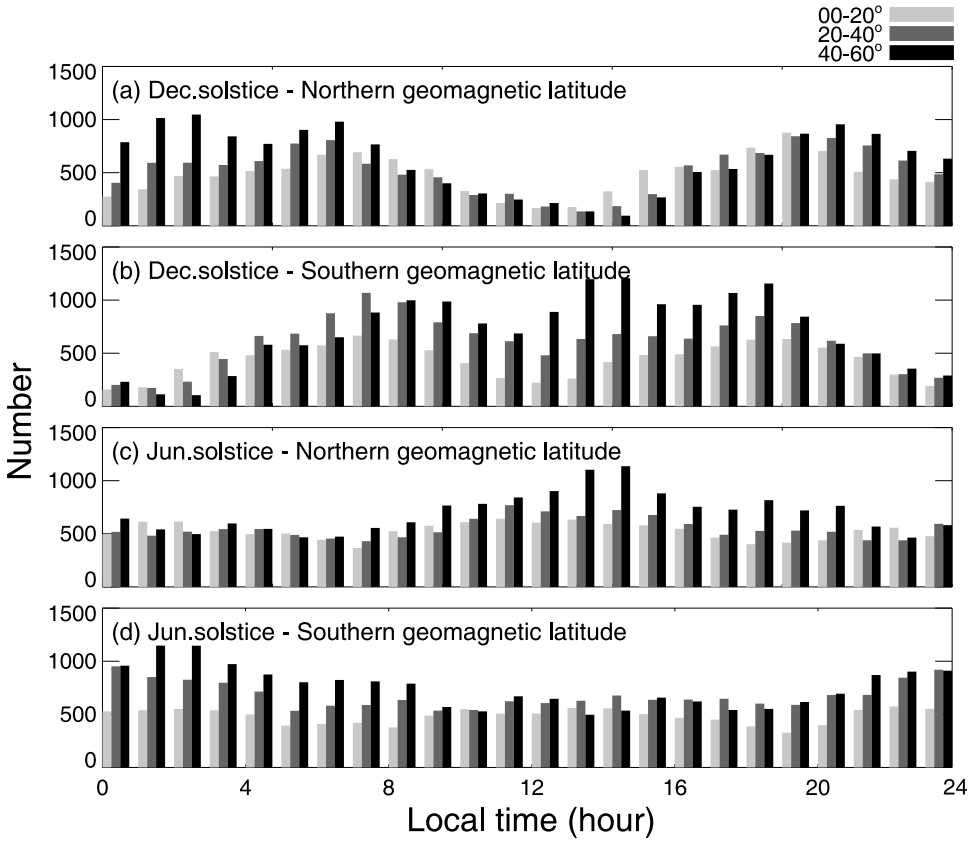

Figure 1. Constellation Observing System for Meteorology, Ionosphere, and Climate (COSMIC) data distribution as a function of local time and magnetic latitude during the (a, b) December and (c, d) June solstices. Data numbers are longitudinally integrated.

Müller-Wodarg [2006] reported higher AI index during solar maximum than during solar minimum. The derived AI index is variable depending on various factors, including ionospheric parameters (e.g., NmF_2, TEC), their measurement techniques, and the selection of the local time, latitude, and longitude ranges. Analysis of longer-term COSMIC data may enable a more rigorous investigation of the dependence of the annual anomaly on solar activity.

[12] At 500 km altitude (Figures 2d and 2e), the electron density at low latitudes is higher during the December solstice than during the June solstice. The northern and southern EIAs are not separable at this altitude. The *F*-peak height is below 300 km during daytime (see Figure 5), and the observations at an altitude of 500 km represent the topside ionospheric morphology. The topside plasma density is greater in the summer hemisphere than in the winter hemisphere; thus the behavior of the electron density at 500 km is not anomalous. The different behavior of the ionosphere at the *F* peak and topside has been identified in various observations [*Balan et al.*, 1997, 2000; *Su et al.*, 1998; *Bailey et al.*, 2000; *Kawamura et al.*, 2000, 2002; *Kil et al.*, 2006; *Liu et al.*, 2007a, 2007b]. As we show in Figure 5 the electron density below the *F* peak at middle latitudes is also greater during summer than during winter.

[13] Longitudinal variation of the winter anomaly feature at middle latitudes is examined using the mean NmF_2 during 1000–1500 LT. The percentage difference in NmF_2 between the December and the June solstices, (DEC–JUN)/DEC, is presented in Figure 3. In Figure 3a the squares (blue) represent the mean density at 40°–60° southern magnetic latitudes, and the asterisks (red) represent the mean density at 40°–60° northern magnetic latitudes. Vertical bars are the standard deviations. Figure 3b presents the median values with the lower (25%) and higher (75%) quartiles (dotted lines). Locations of the northern and southern magnetic poles in 2007 are indicated by the dotted red line (236.8°E) and the dotted blue line (137.6°E), respectively. The good agreement of the mean and median values may indicate that the nonuniform distribution of the COSMIC data during December solstice does not cause a serious bias to our results. The longitudinal variation of the NmF_2 difference between the December and the June solstices shows a dependence on the location of the magnetic poles. At the southern magnetic latitude (blue square), the percentage difference in NmF_2 is smaller at longitudes closer to the southern magnetic pole (although its minimum does not exactly match the location of the southern magnetic pole). A similar trend in the association with the location of the northern magnetic pole is observed at the northern magnetic latitude (red asterisks). Note that regions with smaller values of the percentage difference in NmF_2 at southern magnetic latitude and regions with larger values of it at northern magnetic latitude are more likely to occur for the winter anomaly. Along that line, the winter anomaly is more likely to occur in regions whose longitude is closer to the magnetic poles (southern magnetic pole at southern magnetic latitude

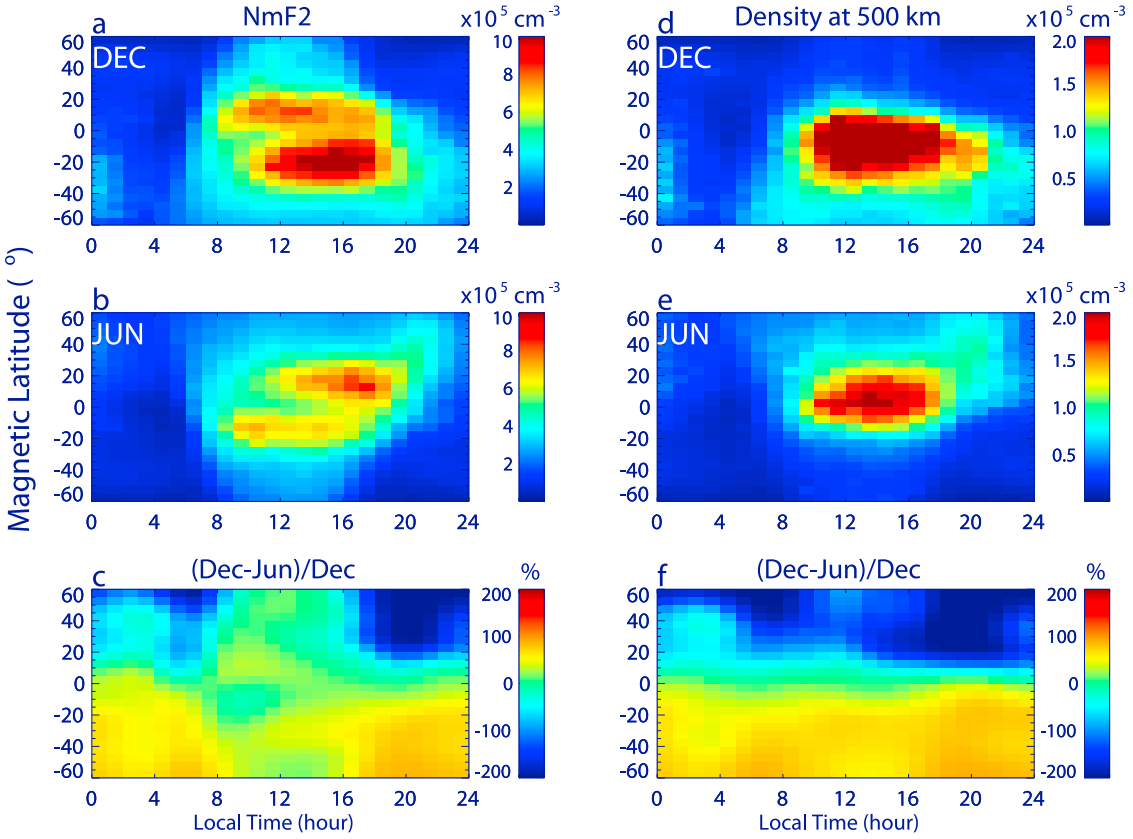

Figure 2. Diurnal and latitude variations of the longitude-mean electron density during the December and June solstices in 2007 observed by COSMIC. (a) NmF_2 during the December solstice. (b) NmF_2 during the June solstice. (c) NmF_2 difference between the December and the June solstices normalized by the NmF_2 during the December solstice. (d–f) The same for the electron density at 500 km altitude. Note the different density scales in the left and right columns.

and northern magnetic pole at northern magnetic latitude). Our result is consistent with previous studies [*Torr and Torr*, 1973; *Rishbeth*, 1998] that showed the occurrence of the winter anomaly in the longitude region close to the magnetic pole during a period of low solar activity. Observation of the similar behavior of the percentage NmF_2 difference in 2008 (data not shown) indicates that the longitudinal variation of the winter anomaly feature identified in Figure 3 is realistic.

[14] The dependence of the intensity of the winter anomaly on the location of the magnetic pole is explained by the dependence of the thermospheric neutral composition on the location of the magnetic pole. Convergence of the poleward wind induced by the summer-to-winter wind circulation and the equatorward wind induced by the heating of auroral region causes a downwelling of atmosphere in middle latitudes of the winter hemisphere. Downwelling of atmosphere and its resulting effect (increase in O/N_2 ratio) are stronger in the longitude region close to the magnetic pole than in the longitude region far from the magnetic pole [*Millward et al.*, 1996; *Rishbeth*, 1998]. In the longitude region close to the magnetic pole the effect of neutral composition on the plasma density is more significant than the effect of solar zenith angle during winter [*Rishbeth*, 1998].

[15] We investigate the variation of electron density profiles with magnetic latitude by using the averaged electron density profiles with magnetic longitude during daytime (1000–1500 LT). Figure 4 shows the electron density profiles during the December (solid line) and June (dashed line) solstices at northern (a) and southern (b) magnetic latitudes. The magnetic latitude increases from left to right. At the northern magnetic latitudes the transition height (the height in the topside where the electron densities during the June and December solstices reverse) decreases with an increase in latitude. Decrease in the F-peak height toward the poles can be explained by the effect of poleward wind during the daytime. The decrease in the transition height with latitude is related to the decrease in the F-peak height in both seasons. A greater electron density in the winter than in the summer occurs in a narrow altitude range near the F-peak height at northern middle latitudes. The electron density is greater overall during the December solstice than during the June solstice at southern middle latitudes.

[16] The behavior of the electron density with altitude and local time is presented in Figure 5. The longitudinal mean vertical electron density profiles are obtained for each hour bin by using the data for the 40°–60° northern (Figures 5a and 5b) and southern (Figures 5c and 5d) magnetic latitudes. Dashed white lines indicate the F-peak height. Focusing on the region near the F-peak height during daytime, we find that the electron density is greater during the December solstice (Figures 5a and 5c) than during the June

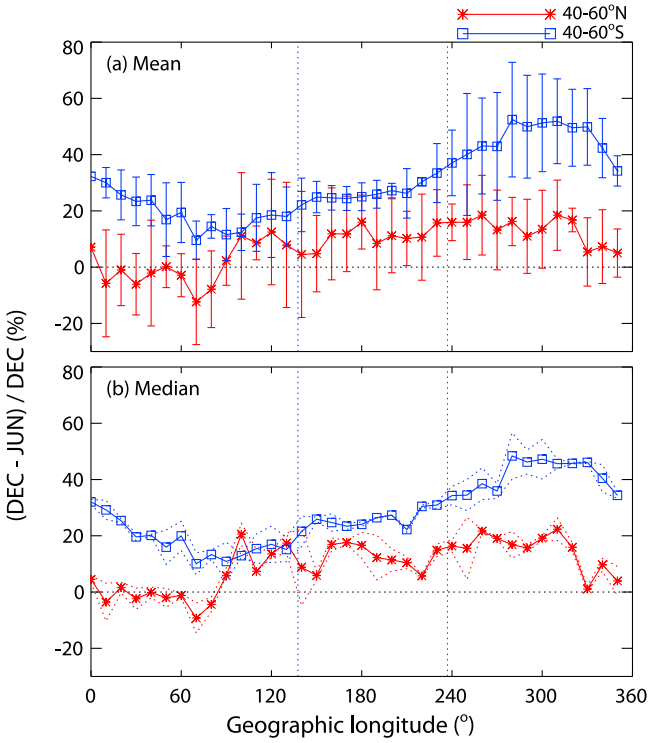

Figure 3. Longitudinal variation in the daytime winter anomaly indicator, (DEC–JUN)/JUN, observed by COSMIC. (a) The mean NmF_2 for each longitude bin is calculated using data at 1000–1500 LT and 40°–60°S (blue squares) and 40°–60°N (red asterisks) at magnetic latitude. Vertical bars are standard deviations. Locations of magnetic poles in Northern and Southern Hemispheres are indicated by the dotted red line (276.8°E) and dotted blue line (137.6°E), respectively. (b) Median NmF_2 with the same format. Dotted lines indicate the lower (25%) and higher (75%) quartiles, respectively.

solstice (Figures 5b and 5d) in both hemispheres. At northern middle latitudes (Figures 5a and 5b) the electron density is greater overall during the June solstice than during the December solstice, if the winter anomaly feature near the *F*-peak height is ignored. Therefore, the seasonal anomalous behavior is a phenomenon only near the *F*-peak height in the Northern Hemisphere. MU radar observations at Shigaraki show similar altitude variation of electron density during solstices at northern middle latitude [*Balan et al.*, 1997, 2000; *Kawamura et al.*, 2002]; the electron density is higher in summer that in winter above 350 km. At southern middle latitudes (Figures 5c and 5d) the seasonal difference in electron density is much more pronounced compared to that at northern middle latitudes. The electron density higher during the December solstice than during the June solstice at all local times and altitude ranges. The winter anomaly feature is not seen at southern middle latitudes.

[17] We note that the absence of the winter anomaly feature at southern middle latitudes is based on the mean behavior of the middle-latitude ionosphere during the solar minimum period. *Pavlov and Pavlova* [2009] reported that the winter anomaly in NmF_2 has been seen in the Southern Hemisphere (Argentine Islands) during periods of low solar activity. Their result, obtained by comparing the NmF_2 during summer and winter under the same solar flux conditions, shows that the occurrence probability of the winter anomaly (winter/summer NmF_2 ratio > 1) is >8% during periods of low solar activity ($F_{10.7}$ < 100). The percentage occurrence of the winter anomaly increases with an increase in solar activity. The result of *Pavlov and Pavlova* [2009] indicates that the occurrence of the winter anomaly is variable from hour to hour or day to day. However, we point out that the winter anomaly features observed for a few days within a period of a month can be caused by the day-to-day variation in the ionosphere. The mechanism that causes the day-to-day variation can be different from the mechanism that causes the winter anomaly. The winter anomaly phenomenon describes the monthly or seasonal behavior of the ionosphere. Our study, based on the seasonal mean plasma density, does not detect the day-to-day variability of the winter anomaly but properly describes the seasonal mean behavior of the ionosphere.

[18] The height of the *F* peak is greater at night than during the day in both hemispheres. The wind component parallel to the magnetic field obtained from Horizontal Wind Model 93 (HWM93) [*Hedin et al.*, 1996] shows that the wind at middle latitude is equatorward during approximately 1800–0600 LT in both hemispheres. The observations from MU radar show seasonal wind patterns similar to those observed by HWM93 [*Kawamura et al.*, 2000, 2002]. Equatorward wind raises the *F*-layer height, but the *F*-layer height also rises at night owing to the loss of oxygen ions even in the absence of the equatorward wind. Loss of oxygen ions by reaction with molecular gases ($O^+ + N_2 \rightarrow NO^+ + N$, $O^+ + O_2 \rightarrow O_2^+ + O$) and subsequent dissociative recombination of molecular ions ($NO^+ + e \rightarrow N + O$, $O_2^+ + e \rightarrow O + O$) occur faster at lower altitudes owing to an increase in molecular gases with decreasing altitude. Faster loss of oxygen ions at lower altitudes, in the absence of photoionization, gives an effect of the *F*-peak height increase.

[19] An interesting feature during the June solstice (Figure 5b) is the occurrence of the electron density peak near 2000 LT. This phenomenon is not explained by the chemical process because, as already described, the increase in the *F*-peak height owing to the chemical process accompanies the electron density decrease in the *F*-peak height. Equatorward wind is the likely mechanism of the electron density increase around 2000 LT. The *F* region at northern middle latitudes is still in the sunlit side at 2000 LT during the June solstice. In the presence of photoionization, uplift of the ionosphere by equatorward wind causes a significant increase in electron density due to a reduction in the recombination reaction rate between O^+ and molecular gases. The situation is different during winter. The electron density increase at night is not seen during the December solstice (Figure 5a). The *F* region at northern middle latitudes is on the darkside before 1800 LT during the December solstice. In the absence of photoionization, uplift of the ionosphere by equatorward wind does not cause a significant increase in electron density. At southern middle latitudes the electron density increase around 2000 LT is not obvious during the summer (December solstice) (Figure 5c). The premidnight electron density increase during summer may be invisible at southern middle latitudes owing to the predominant electron density during daytime. However, we

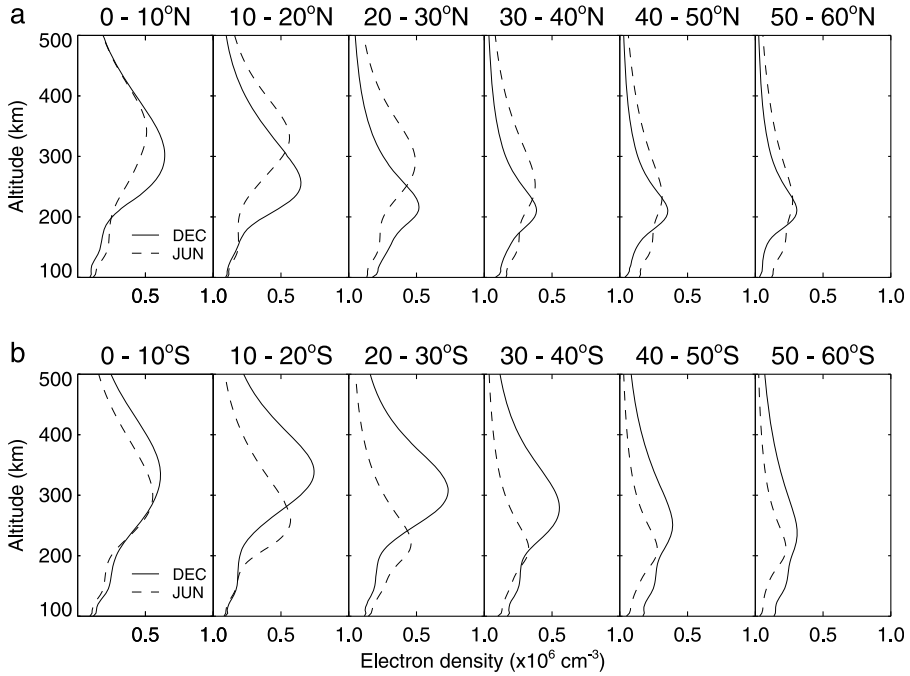

Figure 4. Latitude variation of longitude-mean electron density profiles in the (a) Northern and (b) Southern Hemispheres observed by COSMIC. Mean vertical electron density profiles for each latitude bin are calculated using data at 1000–1500 LT. Electron density profiles during the December and June solstices are represented by solid and dashed lines, respectively.

cannot rule out a hemispheric difference in the nighttime ionosphere. We note that the nighttime electron density at middle latitudes is largely variable with longitude [*Horvath and Essex*, 2003; *Horvath*, 2006; *Luan et al.*, 2008; *Jee et al.*, 2009; *Lin et al.*, 2009]. For further discussion of the variability of the nighttime middle-latitude ionosphere, the reader is referred to the references cited here.

[20] We compare the seasonal behavior of NmF_2 observed by COSMIC with the ionosonde data. Figure 6a shows the locations of the selected ionosonde stations: Wakkanai (141.7°E, 45.4°N), Dyess (260.3°E, 32.5°N), Camden (150.7°E,

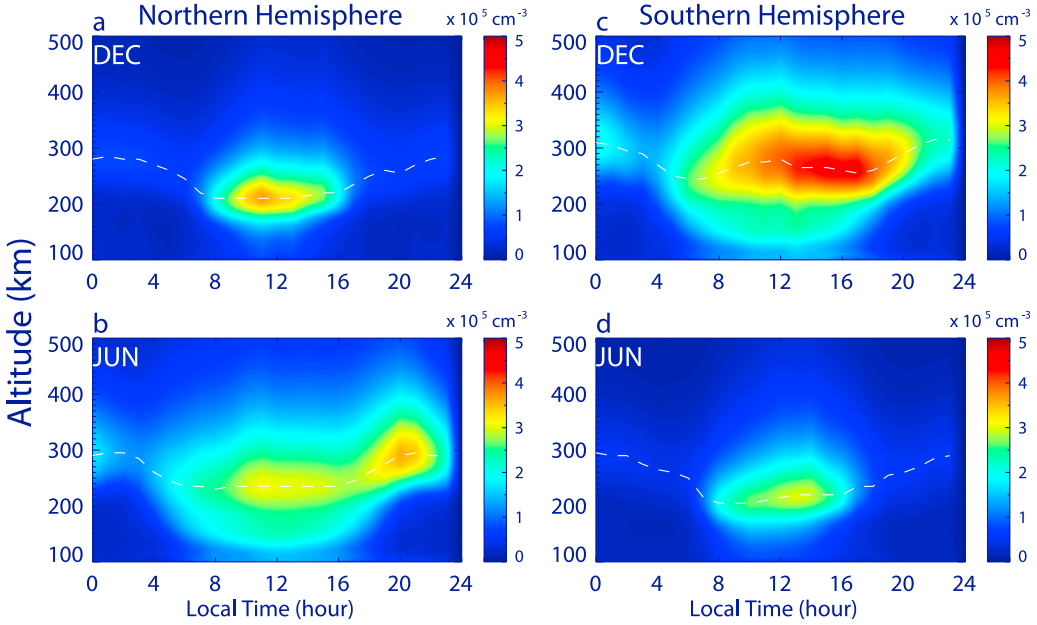

Figure 5. Diurnal and altitude variations of the longitude-mean electron density at middle latitudes observed by COSMIC. Observations in (a, b) the Northern Hemisphere and (c, d) the Southern Hemisphere during the December and June solstices. Dashed white lines indicate the *F*-peak height.

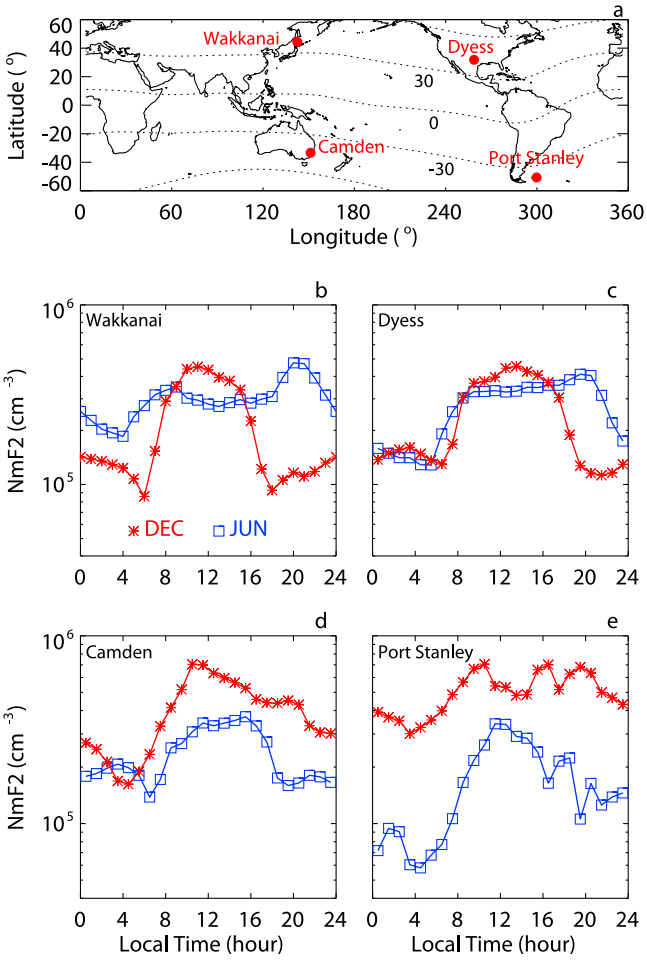

Figure 6. Seasonal and diurnal variations in NmF_2 at middle latitudes observed by ionosondes in 2007. (a) Locations of ionosonde stations. NmF_2 data at (b) Wakkanai, (c) Dyess, (d) Camden, and (e) Port Stanley. NmF_2 data during the December and June solstices are represented by red asterisks and blue squares, respectively.

34.0°S), and Port Stanley (302.2°E, 51.7°S). Magnetic latitudes are shown by dotted lines at 30° intervals. Stations in the Northern and Southern Hemispheres are approximately magnetic conjugates. Mean NmF_2 values during the June (June and July 2007) and December (January and December 2007) solstices are shown by blue squares and red asterisks, respectively. At the northern stations (Figures 6b and 6c), the NmF_2 is greater during the December solstice (winter) than during the June solstice (summer) between 0800 and 1600 LT. The local time range during which the winter anomaly feature occurs is consistent with the observations by COSMIC. The occurrence of the NmF_2 peak near 2000 LT during the June solstice at the northern stations is also consistent with COSMIC observations. At the southern stations (Figures 6d and 6e) the NmF_2 is greater during the December solstice (summer) than during the June solstice (winter) at all local times except for a few hours early in the morning at Camden. We investigated the local time variation of the ionosonde NmF_2 at Camden and Port Stanley during the solar maximum period (year 2001; results not presented). The winter anomaly feature did not appear at Port Stanley at any local time, but a weak winter anomaly appeared during daytime at Camden. The winter anomaly at the northern stations was more pronounced during the solar maximum period than during the solar minimum period, consistent with previous observations [*Yonezawa and Arima*, 1959; *Yonezawa*, 1971, 1972; *Torr and Torr*, 1973].

4. Discussion

[21] The seasonal variation of the thermospheric neutral composition has been suggested to be the major source of the winter anomaly [*Rishbeth and Setty*, 1961; *Duncan*, 1969; *Lumb and Setty*, 1976; *Balan et al.*, 1998; *Rishbeth*, 1998; *Rishbeth and Müller-Wodarg*, 1999, 2006; *Rishbeth et al.*, 2000, 2004; *Yu et al.*, 2004]. Upwelling of the atmosphere in summer and downwelling in winter and the summer-to-winter wind circulation induce different thermospheric neutral compositions between summer and winter. In summer an increase in molecular gases in the *F* region owing to upwelling increases the reaction of O^+ with molecular gases, resulting in a plasma density decrease. The opposite process occurs in winter, resulting in a plasma density increase. The seasonal variation in the number density of the vibrationally excited molecular gases (N_2 and O_2) and electronically excited O^+ also contributes to the generation of the winter anomaly [*Thomas*, 1968; *Strobel and McElroy*, 1970; *Torr et al.*, 1980; *Pavlov and Pavlova*, 2005]. An increase in vibrationally excited molecular gases causes a plasma density decrease because the reaction rate of O^+ with vibrationally excited molecular gases is much faster than the reaction rate with unexcited molecular gases. The production rate of vibrationally excited molecular gases owing to collisions of unexcited N_2 and O_2 with thermal electrons increases with an increase in electron temperature [*Pavlov*, 1998]. Because the electron temperature is higher in summer than in winter, the number density of vibrationally excited molecular gases in summer exceeds that in winter. Both the neutral composition and the population of vibrationally excited molecular gases vary with solar cycle, and therefore, the intensity of the winter anomaly is dependent on the solar cycle.

[22] COSMIC observations show that the daytime electron density at middle latitudes is greater in summer than in winter in both hemispheres except for the winter anomaly feature in the Northern Hemisphere. The observation made by MU radar at northern middle latitudes also shows that the daytime electron density is greater during summer than during winter except for the electron density near the *F*-peak height [*Kawamura et al.*, 2000]. The parameter that may explain the greater electron density in summer than in winter in both hemispheres is the solar zenith angle. In summer the effects of the solar zenith angle and annual anomaly are out of phase in the Northern Hemisphere, whereas they are in phase in the Southern Hemisphere. As a result, the seasonal difference in electron density is much more pronounced in the Southern Hemisphere than in the Northern Hemisphere. The winter anomaly feature may not appear at southern middle latitudes if the harmonic effects of the annual anomaly and solar zenith angle produce a predominantly greater electron density during the December solstice (summer) than during the June solstice (winter).

[23] Note that the dependence of the electron density on the solar zenith angle is a behavior predicted by the Chapman theory and, therefore, is not an anomalous behavior. The exception to this seasonal behavior of the electron density is the winter anomaly feature at northern middle latitudes. The occurrence of a greater NmF_2 during the December solstice than during the June solstice is consistent with the prediction of the effect of neutral composition already described. The question is why the seasonal behavior of the ionosphere near the *F*-peak height is different from the behavior below and above the *F* peak. *Balan et al.* [2000] suggested that the winter anomaly does not appear in the topside because the effect of neutral wind is more significant than the effect of neutral composition in the topside. However, there was no explanation for the different seasonal behaviors of electron density in the lower *F* region and at *F*-peak height. In addition to the chemical processes associated with seasonal variations of solar flux, solar zenith angle, and neutral composition, dynamic processes (plasma transport by electric fields and neutral winds) may play a role in the concentration of plasma in a narrow altitude range. Neutral winds are an important source of the seasonal and hemispheric variations in electron density, especially in the topside [e.g., *Su et al.*, 1998; *Kawamura et al.*, 2002]. Although the effect of the vertical $\mathbf{E} \times \mathbf{B}$ drift on the winter anomaly has not yet been considered seriously, any seasonal and hemispheric differences in vertical $\mathbf{E} \times \mathbf{B}$ drift and the combination of the effect of vertical $\mathbf{E} \times \mathbf{B}$ drift with the effect of neutral winds will affect the formation of the winter anomaly.

5. Conclusions

[24] We have investigated the seasonal behavior of the middle-latitude ionosphere by analyzing COSMIC radio occultation data during a near-solar-minimum period (year 2007). The COSMIC observation identifies an occurrence of the winter anomaly feature during 0800–1600 LT in the Northern Hemisphere but not in the Southern Hemisphere. The intensity of the winter anomaly shows longitudinal variation, and a more intense winter anomaly is likely to occur in the longitude region closer to the magnetic pole. Except for the winter anomaly feature near the *F*-peak height in the Northern Hemisphere, the seasonal behavior of the middle-latitude ionosphere (occurrence of greater electron density in summer than in winter) conforms to the prediction using the solar zenith angle. The absence of the winter anomaly in the Southern Hemisphere could be due to either the weakening of the winter anomaly or the dominant effect of the annual anomaly during a solar minimum period. Analysis of COSMIC data collected during a broader period of the solar cycle may provide further insight into the relationship between the annual and the winter anomalies during a solar cycle.

[25] **Acknowledgments.** This work was funded by the Korea Meteorological Administration Research and Development Program under grant CATER 2006-3104. H. Kil acknowledges support from NASA grant NNX08AQ12G. Q. Wu acknowledges support from NSF grant ATM 0640745 and NASA grant NNX09AG64G. NCAR is supported by the National Science Foundation. Wakkanai ionosonde data were provided by the WDC for Ionosphere in Tokyo, located at the National Institute of Information and Communications Technology.

[26] Robert Lysak thanks the reviewers for their assistance in evaluating the manuscript.

References

Alcaydé, D., P. Bauer, and J. Fontanari (1974), Long-term variations of thermospheric temperature and composition, *J. Geophys. Res.*, *79*(4), 629–637.

Bailey, G. J., Y. Z. Su, and K.-I. Oyama (2000), Yearly variations in the low-latitude topside ionosphere, *Ann. Geophys.*, *18*, 789–798.

Balan, N., Y. Otsuka, and S. Fukao (1997), New aspects in the annual variation of the ionosphere observed by the MU radar, *Geophys. Res. Lett.*, *24*, 2287–2290.

Balan, N., Y. Otsuka, G. Bailey, and S. Fukao (1998), Equinoctial asymmetries in the ionosphere and thermosphere observed by the MU radar, *J. Geophys. Res.*, *103*(A5), 9481–9495.

Balan, N., Y. Otsuka, S. Fukao, M. A. Abdu, and G. J. Bailey (2000), Annual variations of the ionosphere: A review based on MU radar observations, *Adv. Space Res.*, *25*(1), 153–162.

Berkner, L. V., and H. W. Wells (1938), Non-seasonal change of F2-region ion density, *Terr. Magn. Atmos. Electr.*, *43*, 15–36.

Duncan, R. A. (1969), *F*-region seasonal and magnetic storm behavior, *J. Atmos. Terr. Phys.*, *31*, 59–70.

Fuller-Rowell, T. (1998), The "thermospheric spoon": A mechanism for the semiannual density variation, *J. Geophys. Res.*, *103*(A3), 3951–3956.

Hedin, A., and D. Alcaydé (1974), Comparison of atomic oxygen measurements by incoherent scatter and satellite-borne mass spectrometer techniques, *J. Geophys. Res.*, *79*(10), 1579–1581.

Hedin, A. E., et al. (1996), Empirical wind model for the upper, middle and lower atmosphere, *J. Atmos. Terr. Phys.*, *58*, 1421–1447.

Horvath, I. (2006), A total electron content space weather study of the nighttime Weddell Sea Anomaly of 1996/1997 southern summer with TOPEX/Poseidon radar altimetry, *J. Geophys. Res.*, *111*, A12317, doi:10.1029/2006JA011679.

Horvath, I., and E. A. Essex (2003), The Weddell Sea Anomaly observed with the TOPEX satellite data, *J. Atmos. Terr. Phys.*, *65*, 693–706.

Jee, G., R. W. Schunk, and L. Scherliess (2004), Analysis of TEC data from the TOPEX/Poseidon mission, *J. Geophys. Res.*, *109*, A01301, doi:10.1029/2003JA010058.

Jee, G., A. G. Burns, Y.-H. Kim, and W. Wang (2009), Seasonal and solar activity variations of the Weddell Sea Anomaly observed in the TOPEX total electron content measurements, *J. Geophys. Res.*, *114*, A04307, doi:10.1029/2008JA013801.

Kawamura, S., Y. Otsuka, S.-R. Zhang, S. Fukao, and W. Oliver (2000), A climatology of middle and upper atmosphere radar observations of thermospheric winds, *J. Geophys. Res.*, *105*(A6), 12777–12788.

Kawamura, S., N. Balan, Y. Otsuka, and S. Fukao (2002), Annual and semiannual variations of the midlatitude ionosphere under low solar activity, *J. Geophys. Res.*, *107*(A8), 1166, doi:10.1029/2001JA000267.

Kil, H., R. DeMajistre, L. J. Paxton, and Y. Zhang (2006), Nighttime *F*-region morphology in the low and middle latitudes seen from DMSP F15 and TIMED/GUVI, *J. Atmos. Sol. Terr. Phys.*, *68*, 1672–1681.

King, G. (1961), The seasonal anomalies in the *F* region, *J. Geophys. Res.*, *66*(12), 4149–4154.

King, G. A. M. (1964), The dissociation of oxygen and high level circulation in the atmosphere, *J. Atmos. Sci.*, *21*(3), 201–237.

Lee, W. K., J. K. Chung, S. Cho, J. U. Park, J. H. Cho, J. C. Yoon, J. H. Lee, and S. R. Lee (2007), Retrieval of electron density profile for KOMPSAT-5 GPS radio occultation data processing system, *J. Astron. Space. Sci*, *24*(4), 297–308.

Lei, J., et al. (2007), Comparison of COSMIC ionospheric measurements with ground-based observations and model predictions: Preliminary results, *J. Geophys. Res.*, *112*, A07308, doi:10.1029/2006JA012240.

Lin, C. H., J. Y. Liu, C. Z. Cheng, C. H. Chen, C. H. Liu, W. Wang, A. G. Burns, and J. Lei (2009), Three-dimensional ionospheric electron density structure of the Weddell Sea Anomaly, *J. Geophys. Res.*, *114*, A02312, doi:10.1029/2008JA013455.

Liu, L., B. Zhao, W. Wan, S. Venkatraman, M.-L. Zhang, and X. Yue (2007a), Yearly variations of global plasma densities in the topside ionosphere at middle and low latitudes, *J. Geophys. Res.*, *112*, A07303, doi:10.1029/2007JA012283.

Liu, L., W. Wan, X. Yue, B. Zhao, B. Ning, and M.-L. Zhang (2007b), The dependence of plasma density in the topside ionosphere on solar activity level, *Ann. Geophys.*, *25*(6), 1337–1343.

Liu, L., B. Zhao, W. Wan, B. Ning, M.-L. Zhang, and M. He (2009), Seasonal variations of the ionospheric electron densities retrieved from Constellation Observing System for Meteorology, Ionosphere, and Climate mission radio occultation measurements, *J. Geophys. Res.*, *114*, A02302, doi:10.1029/2008JA013819.

Luan, X., W. Wang, A. Burns, S. C. Solomon, and J. Lei (2008), Mid-latitude nighttime enhancement in *F* region electron density from global COSMIC measurements under solar minimum winter condition, *J. Geophys. Res.*, *113*, A09319, doi:10.1029/2008JA013063.

Lumb, H. M., and C. S. G. K. Setty (1976), The *F*2 layer seasonal anomaly. *Ann. Geophys.*, *32*, 243–256.

Mayr, H. G., I. Harris, and N. W. Spencer (1978), Some properties of upper atmosphere dynamics, *Rev. Geophys. Space Phys.*, *16*, 539–565.

Mendillo, M., C. Huang, X. Pi, H. Rishbeth, and R. Meier (2005), The global ionospheric asymmetry in total electron content, *J. Atmos. Sol. Terr. Phys.*, *67*, 1377–1387.

Millward, G., H. Rishbeth, T. Fuller-Rowell, A. Aylward, S. Quegan, and R. Moffett (1996), Ionospheric F_2 layer seasonal and semiannual variations, *J. Geophys. Res.*, *101*(A3), 5149–5156.

Oliver, W. L., S. Kawamura, and S. Fukao (2008), The causes of midlatitude F layer behavior, *J. Geophys. Res.*, *113*, A08310, doi:10.1029/2007JA012590.

Pavlov, A. V. (1998), The role of vibrationally excited oxygen and nitrogen in the ionosphere during the undisturbed and geomagnetic storm period of 6–12 April 1990, *Ann. Geophys.*, *16*, 589–601.

Pavlov, A. V., and N. M. Pavlova (2005), Causes of the mid-latitude NmF2 winter anomaly, *J. Atmos. Sol. Terr. Phys.*, *67*, 862–877.

Pavlov, A. V., and N. M. Pavlova (2009), Anomalous variations of NmF2 over the Argentine Islands: A statistical study, *Ann. Geophys.*, *27*, 1363–1375.

Pavlov, A. V., N. M. Pavlova, and S. F. Makarenko (2010), A statistical study of the mid-latitude *Nm*F2 winter anomaly, *Adv. Space Res.*, *45*(3), 374–385.

Rishbeth, H. (1998), How the thermospheric circulation affects the ionosphere, *J. Atmos. Sol. Terr. Phys.*, *60*, 1385–1402.

Rishbeth, H., and I. C. F. Müller-Wodarg (1999), Vertical circulation and thermospheric composition: a modeling study, *Ann. Geophys.*, *17*, 794–805.

Rishbeth, H., and I. C. F. Müller-Wodarg (2006), Why is there more ionosphere in January than in July? The annual asymmetry in the F_2 layer, *Ann. Geophys.*, *24*, 3293–3311.

Rishbeth, H., and C. S. G. K. Setty (1961), The *F*-layer at sunrise, *J. Atmos. Terr. Phys.*, *21*, 263–276.

Rishbeth, H., I. C. F. Müller-Wodarg, L. Zou, T. J. Fuller-Rowell, G. H. Millward, R. J. Moffett, D. W. Idenden, and A. D. Aylward (2000), Annual and semiannual variations in the ionospheric F_2 layer: II. Physical discussion, *Ann. Geophys.*, *18*, 945–956.

Rishbeth, H., R. A. Heelis, and I. C. F. Müller-Wodarg (2004), Variations of thermospheric composition according to AE-C data and CTIP modeling, *Ann. Geophys.*, *22*, 441–452.

Strobel, D. F., and M. B. McElroy (1970), The *F*2 layer at middle latitudes, *Planet. Space Sci.*, *18*, 1181–1202.

Su, Y. Z., G. J. Bailey, and K.-I. Oyama (1998), Annual and seasonal variations in the low-latitude topside ionosphere, *Ann. Geophys.*, *16*, 974–985.

Thomas, G. K. (1968), The effect of diurnal temperature changes on the *F*2 layer: II. Temperature dependent loss rate, *J. Atmos. Terr. Phys.*, *30*, 1429–1437.

Titheridge, J. E., and M. J. Buonsanto (1983), Annual variations in the electron content and height of the *F* layer in the northern and Southern Hemispheres, related to neutral compositions, *J. Atmos. Terr. Phys.*, *45*, 683–696.

Torr, M. R., and D. G. Torr (1973), The seasonal behaviour of the *F*2-layer of the ionosphere, *J. Atmos. Terr. Phys.*, *35*, 2237–2251.

Torr, D. G., M. R. Torr, and P. G. Richards (1980), Causes of the *F* region winter anomaly, *Geophys. Res. Lett.*, *7*(5), 301–304.

Yonezawa, T. (1971), The solar-activity and latitudinal characteristics of the seasonal, non-seasonal and semi-annual variations in the peak electron densities of the *F*2-layer at noon and midnight in middle and low latitudes, *J. Atmos. Terr. Phys.*, *33*, 889–907.

Yonezawa, T. (1972), Semi-annual variations in the peak electron densities of the *F*2- and *E*-layers, *J. Radio Res. Labs.*, *19*, 1–22.

Yonezawa, T. and Y. Arima (1959), On the seasonal and non-seasonal annual variations and the semi-annual variation in the noon and midnight electron densities of the *F*2 layer in middle latitudes, *J. Radio Res. Labs.*, *6*, 293–309.

Yu, T., W. Wan, L. Liu, and B. Zhao (2004), Global scale annual and semiannual variations of daytime NmF2 in the high solar activity years, *J. Atmos. Sol. Terr. Phys.*, *66*, 1691–1701.

Zeng, Z., A. Burns, W. Wang, J. Lei, S. Solomon, S. Syndergaard, L. Qian, and Y. H. Kuo (2008), Ionospheric annual asymmetry observed by the COSMIC radio occultation measurements and simulated by the TIEGCM, *J. Geophys. Res.*, *113*, A07305, doi:10.1029/2007JA012897.

Zhao, B., W. Wan, L. Liu, T. Mao, Z. Ren, M. Wang, and A. B. Christensen (2007), Features of annual and semiannual variations derived from the global ionospheric maps of total electron content, *Ann. Geophys.*, *25*, 2513–2527.

Zou, L., H. Rishbeth, I. C. F. Müller-Wodarg, A. D. Aylward, G. H. Millward, T. J. Fuller-Rowell, D. W. Idenden, and R. J. Moffett (2000), Annual and semiannual variations in the ionospheric *F*2-layer: I. Modelling, *Ann. Geophys.*, *18*, 927–944.

S. Cho, Y.-S. Kwak, W. K. Lee, and J. U. Park, Korea Astronomy and Space Science Institute, 776 Daedeokdaero, Yuseong-gu, Daejeon 305-348, Korea. (wklee@kasi.re.kr)

H. Kil, The Johns Hopkins University Applied Physics Laboratory, 11100 Johns Hopkins Rd., Laurel, MD 20723, USA.

Q. Wu, High Altitude Observatory, National Center for Atmospheric Research, PO Box 3000, Boulder, CO 80307, USA.